Received: 16 March 2018 | Revised: 16 October 2018 | Accepted: 17 October 2018

DOI: 10.1002/hbm.24447

WILEY

RESEARCH ARTICLE

Partially impaired functional connectivity states between right anterior insula and default mode network in autism spectrum disorder

Xiaonan Guo[1] | Xujun Duan[1] | John Suckling[2] | Heng Chen[1] | Wei Liao[1] | Qian Cui[3] | Huafu Chen[1]

[1]The Clinical Hospital of Chengdu Brain Science Institute, MOE Key Lab for Neuroinformation; School of Life Science and Technology, Center for Information in BioMedicine, University of Electronic Science and Technology of China, Chengdu, People's Republic of China

[2]Department of Psychiatry, Behavioural and Clinical Neuroscience Institute, University of Cambridge; Cambridge and Peterborough NHS Trust, Cambridge, United Kingdom

[3]School of Political Science and Public Administration, University of Electronic Science and Technology of China, Chengdu, People's Republic of China

Correspondence
Huafu Chen, The Clinical Hospital of Chengdu Brain Science Institute, MOE Key Lab for Neuroinformation; School of Life Science and Technology, Center for Information in BioMedicine, University of Electronic Science and Technology of China, Chengdu 610054, People's Republic of China
Email: chenhf@uestc.edu.cn
andXujun Duan, The Clinical Hospital of Chengdu Brain Science Institute, MOE Key Lab for Neuroinformation; School of Life Science and Technology, Center for Information in BioMedicine, University of Electronic Science and Technology of China, Chengdu 610054, People's Republic of China.
Email: duanxujun@uestc.edu.cn

Funding information
Fundamental Research Funds for the Central Universities, Grant/Award Numbers: 2672018ZYGX2018J079, ZYGX2016J187; National Institute for Health Research Cambridge Biomedical Resource Centre; National Natural Science Foundation of China, Grant/Award Numbers: 61533006, 61673089, 81771919, 81871432; Sichuan Science and Technology Program, Grant/Award Number: 2018TJPT0016; Specialized Research Fund for the Doctoral Program of Higher Education of China, Grant/Award Number: 20120185110028

Abstract

Time-invariant resting-state functional connectivity studies have illuminated the crucial role of the right anterior insula (rAI) in prominent social impairments of autism spectrum disorder (ASD). However, a recent dynamic connectivity study demonstrated that rather than being stationary, functional connectivity patterns of the rAI vary significantly across time. The present study aimed to explore the differences in functional connectivity in dynamic states of the rAI between individuals with ASD and typically developing controls (TD). Resting-state functional magnetic resonance imaging data obtained from a publicly available database were analyzed in 209 individuals with ASD and 298 demographically matched controls. A k-means clustering algorithm was utilized to obtain five dynamic states of functional connectivity of the rAI. The temporal properties, frequency properties, and meta-analytic decoding were first identified in TD group to obtain the characteristics of each rAI dynamic state. Multivariate analysis of variance was then performed to compare the functional connectivity patterns of the rAI between ASD and TD groups in obtained states. Significantly impaired connectivity was observed in ASD in the ventral medial prefrontal cortex and posterior cingulate cortex, which are two critical hubs of the default mode network (DMN). States in which ASD showed decreased connectivity between the rAI and these regions were those more relevant to socio-cognitive processing. From a dynamic perspective, these findings demonstrate partially impaired resting-state functional connectivity patterns between the rAI and DMN across states in ASD, and provide novel insights into the neural mechanisms underlying social impairments in individuals with ASD.

KEYWORDS

autism spectrum disorder, default mode network, dynamic functional connectivity, resting-state functional magnetic resonance imaging, right anterior insula, state

1 | INTRODUCTION

Autism spectrum disorder (ASD) is a heterogeneous neurodevelopmental disorder manifested as pervasive impairments in social interaction and communication, along with repetitive and stereotypic behavioral patterns (American Psychiatric Association, 2013). Clinical characteristics among individuals with ASD can vary widely; these characteristics include variable degrees of communication skills, motor abnormalities, intellectual impairments, and a wide range of comorbidities. Social deficits are common symptoms in all ASD types.

Prominent social impairments in ASD encompass multiple forms of impaired social cognitive processes, including failure in establishing or maintaining social reciprocity, deficits in developing body languages or eye contact, and difficulty in understanding intentions, sensations, or emotions of other people and inappropriate self-referential thought. These impairments may be attributed to aberrant social orientation and motivation in individuals with ASD (American Psychiatric Association, 2013; Chevallier, Kohls, Troiani, Brodkin, & Schultz, 2012). In general, individuals with ASD display different preferences to socially salient stimuli spanning faces, eyes, and speech indicating aberrant salience detection processes towards the social world (Ceponiene et al., 2003; Klin, Jones, Schultz, Volkmar, & Cohen, 2002).

As a critical hub of salience network (SN), the anterior insula is traditionally considered the principal brain region for interoceptive processing involved in sensing human physiological states; awareness of self, others, and the environment; experiencing emotions; and interaction with other essential networks, such as the default mode network (DMN) and central executive network (CEN) (Craig, 2009; Menon, 2011; Menon & Uddin, 2010). In particular, the right but not left, anterior insula is suggested to act as a "causal outflow hub" in initiating the switching of large-scale brain networks between internally (e.g., DMN) and externally focused networks (e.g., CEN) during cognitive information processing and the resting state (Menon, 2011; Menon & Uddin, 2010; Sridharan, Levitin, & Menon, 2008; Uddin, 2015; Wang et al., 2018). In addition, the structural integrity of white-matter tracts between the right anterior insula (rAI) and other SN regions is necessary for efficient control of the DMN (Bonnelle et al., 2012). The functional right-hemisphere lateralization of the anterior insula has also been validated during error processing (Ham, Leff, de Boissezon, Joffe, & Sharp, 2013), salience processing (Späti et al., 2014), heartbeat awareness (Critchley, Wiens, Rotshtein, Öhman, & Dolan, 2004), and self-related processing (Devue et al., 2007). Meta-analytic studies characterizing functional diversity across the brain have demonstrated that the rAI is a highly functionally diverse region participating in various task domains while coactivating with a broad set of brain regions (Anderson, Kinnison, & Pessoa, 2013; Uddin, Kinnison, Pessoa, & Anderson, 2013). Therefore, the functional centrality of the rAI may establish its central role in salience processing in the brain.

Socio-cognitive and other impairments in individuals with ASD are increasingly linked to connectivity abnormalities at the whole-brain circuit level, especially in large-scale brain networks (Doyle-Thomas et al., 2015; Guo et al., 2016; Khan et al., 2015; Nomi & Uddin, 2015). Among multiple brain regions characterized as the key structures in ASD development, prior neuroimaging literature support the vital role of the rAI in neural substrates underlying social dysfunctions in ASD (Di Martino et al., 2009; Uddin & Menon, 2009). Convergent hypoactivity was identified in the rAI in individuals with ASD during various social tasks (Di Martino et al., 2009). This has shed light on the potential relationship between functional alterations of the rAI and social deficits in individuals with ASD. Another recent neuroimaging study reported that during social and nonsocial attention tasks, children with ASD exhibited different multivariate spatial activation patterns of the rAI from those of typically developing peers (Odriozola et al., 2015). These children also manifested atypical connectivity patterns in the same region while processing socially deviant stimuli compared with nonsocially deviant stimuli (Odriozola et al., 2015). Aligned with the task-based evidence on abnormalities in the rAI in ASD, resting-state functional connectivity studies have also underscored altered functional circuits of this structure in relation to autistic symptoms in the social domain. Children and adolescents with ASD exhibited intrinsic underconnectivity between the rAI and temporal and dorsolateral prefrontal regions, and posterior cingulate cortex (PCC), a primary node for the DMN (Abbott et al., 2016). Interestingly, significant negative correlation between functional connectivity within the SN and social deficits in individuals with ASD was absent in the control group (Abbott et al., 2016). This finding indicates the specific role of the SN in the predominant impairments of social behaviors in ASD. Decreased intrinsic functional connectivity was also demonstrated between the rAI and amygdala in high-functioning autistic individuals between 12 and 20 years of age (Ebisch et al., 2011). This result highlights altered detection of emotional valence and impaired ability to understand mental states of the self and others in ASD. Furthermore, a hypoconnectivity pattern was identified within and between brain networks associated with social processing in ASD (von dem Hagen, Stoyanova, Baron-Cohen, & Calder, 2012). This hypoconnectivity included reduced intrinsic connectivity between the rAI and several critical hubs of DMN including the medial prefrontal cortex (mPFC) and angular gyrus. These brain imaging studies across various social tasks and during the resting state convergently indicate that altered rAI activity and functional connectivity in ASD is likely to be associated with prominent social impairments. These findings further demonstrated the importance of investigating the rAI to facilitate our understanding of the neural mechanisms underlying ASD.

Resting-state functional magnetic resonance imaging (fMRI) studies have shaped our understanding of the temporal correlations of spatially distributed brain regions, described as intrinsic connectivity networks in the absence of tasks or stimuli (Biswal et al., 2010; Biswal, Zerrin Yetkin, Haughton, & Hyde, 1995; Fox et al., 2005). These correlations are based on the assumption that spatiotemporal organization of spontaneous brain activity is stationary over the measurement period. With this hypothesis, traditional functional connectivity approaches obtain a static connectivity pattern of coherent fluctuations by estimating functional connectivity across an entire resting-state acquisition. Recent advances in neuroimaging have revealed that functional connectivity among brain regions exhibits meaningful variations over time, implicating the dynamic properties of resting-state functional connectivity (Hutchison et al., 2013; Li et al., 2018; Preti, Bolton, & Ville, 2016). A considerable number of analysis strategies has been applied to capture the time-varying patterns of resting-state functional connectivity (Hutchison et al., 2013; Khambhati, Sizemore, Betzel, & Bassett, 2017; Preti et al., 2016). Among these approaches, some dynamic functional connectivity (dFC) studies demonstrate the time-varying dynamic interplay among brain regions, and identified recurring functional connectivity patterns, called "dFC states" (Allen et al., 2014; Calhoun, nbsp, Robyn, et al., 2014; Preti et al., 2016). Typically developing individuals exhibit highly flexible dFC states between the rAI and other brain regions throughout the resting state (Nomi et al., 2016). Applying the dFC approach to neuropsychiatric disorders has illustrated the clinical potential of dFC states in

illuminating complex, flexible neural mechanisms. For instance, previous dFC studies in schizophrenia demonstrated that pathological alterations are only present in some dynamic states (Damaraju et al., 2013; Du et al., 2016). Similar dFC studies in epilepsy revealed state-specific impairments of functional connectivity patterns in participants with epilepsy compared with healthy controls (Liao, Zhang, et al., 2014; Liu et al., 2016). Individuals with ASD were also confirmed to exhibit abnormal temporal variability in functional architecture at rest (Falahpour et al., 2016; He et al., 2018; Zhang et al., 2016). Several studies have examined functional connectivity profiles of the rAI at rest in ASD (Abbott et al., 2016; Ebisch et al., 2011; von dem Hagen et al., 2012). However, to the best of our knowledge, none of these has considered the dynamic nature of synchronous fluctuations while exploring the changes of functional connectivity patterns of the rAI in ASD.

In the present study, we utilized a large, multisite, resting-state fMRI dataset from the open-access Autism Brain Imaging Data Exchange (ABIDE, http://fcon_1000.projects.nitrc.org/indi/abide/) repository to examine the possible differences in functional connectivity in dynamic states of the rAI between ASD and typically developing controls (TD) groups (Di Martino et al., 2014). Given that the dynamic states are obtained by a data-driven approach, it is worthwhile to first specify their characteristics. The current study aimed to answer two questions: (a) what are the characteristics of these dFC states of the rAI? and (b) is there any difference between ASD and TD groups in functional connectivity patterns in different dynamic states? Therefore, we first analyzed the temporal properties, frequency properties, and the potential psychological and physiological processes of dynamic states in TD group. Then, we compared functional connectivity patterns between ASD and TD in five obtained dynamic states. Static functional connectivity studies showed rAI abnormalities in ASD and these connectivity abnormalities play a critical role in social impairments related to the disease (Abbott et al., 2016; Ebisch et al., 2011; von dem Hagen et al., 2012). Thus, we hypothesized that individuals with ASD would exhibit altered functional connectivity between the rAI and social brain regions.

2 | METHODS

2.1 | Participants

Original resting-state fMRI and demographic data were collected from the open-access ABIDE database (Di Martino et al., 2014). Inclusion criteria were the same as Chen, Nomi, Uddin, Duan, and Chen (2017). Briefly, preliminary inclusion criteria of the present study were based on the sample selection procedure of Di Martino et al. (2014) and yielded an initial sample of 763 males (ASD/TD: 360/403) from 17 sites. Second-level inclusion criteria were established to reduce the spurious effects of the potential confounds, such as group-level mismatch on full-scale IQ (FIQ) and framewise displacement (FD) due to the head motion during fMRI acquisition. Analyses were limited to: (a) participants without excessive head motion (i.e., motion within 2 mm translation and 2° rotation and less than 50% frames with large FD, as indicated in *Preprocessing*); (b) participants with complete cortical coverage in the resting-state scan; (c) participants with age within mean ± 3 *SD* across groups; (d) using a data-driven algorithm that maximized *p* values of group differences on age, FIQ, and mean FD (using two sample *t* tests) to create a well-matched dataset of ASD and TD groups. To exclude potential interaction effects induced by sites, we also maximized *p* values of interaction effects between sites and groups on age, FIQ, and mean FD using two-way analysis of variance (ANOVA); and (e) sites with more than five ASD or TD participants remaining after the above-mentioned selection procedure. These criteria yielded a well-matched dataset of 507 individuals (ASD/TD: 209/298) from 14 sites.

Detailed information on diagnostic protocols and ethical statements are publicly available at http://fcon_1000.projects.nitrc.org/indi/abide/. Briefly, all individuals with ASD had a clinical diagnosis of Autistic Disorder, Asperger's Disorder, or Pervasive Developmental Disorder Not-Otherwise-Specified. Individuals with typical development showed no history of neurological or psychiatric disorders. All experimental protocols were approved by the local Institutional Review Boards. Written informed consent/assent was obtained from every participant. Demographic data are summarized in Table 1.

2.2 | Data preprocessing

Resting-state fMRI data were preprocessed using the advanced edition of Data Processing Assistant for Resting-State fMRI (DPARSF A v4.1, http://rfmri.org/DPARSF) (Yan & Zang, 2010). Image preprocessing steps included discarding the first 10 volumes, slice-timing correction, spatial realignment (participants with translational or rotational head motion higher than 2 mm or 2° were excluded), normalization to standard echo-planar imaging template in the Montreal Neurological Institute (MNI) stereotaxic space and resampling to $3 \times 3 \times 3$ mm^3, spatial smoothing (full width at half maximum = 6 mm), the removal of linear trends, despiking by 3dDespike algorithm in Analysis of Functional NeuroImaging (AFNI, https://afni.nimh.nih.

TABLE 1 Demographics and clinical characteristics of the participants

	ASD (*n* = 209)	TD (*n* = 298)	*p* Value
Age	16.5 ± 6.2	16.8 ± 6.2	.5642[a]
Site × group interaction	–	–	.9642[b]
FIQ	110.6 ± 13.4	110.2 ± 11.4	.7191[a]
Site × group interaction	–	–	.8502[b]
Mean FD (mm)	0.14 ± 0.07	0.14 ± 0.07	.7219[a]
Site × group interaction	–	–	.8341[b]
ADOS			
Social subscore	8 ± 3	–	–
Communication subscore	4 ± 1	–	–
RRB subscore	2 ± 1	–	–

ADOS = Autism Diagnostic Observation Schedule (social and communications subscores are available for 131 ASD subjects; RRB subscore is available for 118 ASD subjects); ASD = autism spectrum disorder; FD = framewise displacement; FIQ = the full-scale intelligence quotient; RRB = restricted and repetitive behaviors; TD = typically developing controls.

[a] *p* values for two sample *t* test.

[b] *p* values for analysis of variance (ANOVA).

gov/afni/), nuisance covariates regression (including Friston 24 head motion parameters [Friston, Williams, Howard, Frackowiak, & Turner, 1996; Satterthwaite et al., 2012; Chao-Gan Yan et al., 2013], global signal, the top five principal components from the white matter and cerebrospinal fluid signals by using component-based noise correction [CompCor] method [Behzadi, Restom, Liau, & Liu, 2007]) and band-pass filtering (0.01–0.1 Hz). Given the potential confounding effects of head micromovements on functional connectivity measures (Power, Barnes, Snyder, Schlaggar, & Petersen, 2012), we examined FD values obtained in the realignment of each scan. Time points with FD > 0.5 mm along with the preceding one and the latter two time points were labeled as high-motion frames. Participants with more than 50% high-motion frames were excluded from the analyses. We utilized despiking instead of the "scrubbing" approach (Power et al., 2012) to address the potential motion artifacts without adversely affecting statistical power, as performed in prior studies (Allen et al., 2014; Marusak et al., 2016; Nomi et al., 2016). Signal outliers higher than the median absolute deviation were replaced with the best estimate by using a third-order spline fit to clean portions of the time series. This method retains the temporal information of signals while improving the root-mean-square of temporal derivative of the time courses. Detailed information about head motion is also summarized in Table S1, Supporting Information 1. Average FD and maximum FD values, number of time points with FD > 0.5 mm, percentage of time points with FD > 0.5 mm, within-subject variability of six motion parameters for each participant are provided in Supporting Information 2. Group comparisons on head motion metrics showed no significant difference.

2.3 | Regions of interest selection

Meta-analysis was performed using Neurosynth (http://www.neurosynth.org/) to obtain coordinates of the rAI in the SN (Wager, 2011). We conducted a forward inference analysis of the term "salience network." The resulting statistical inference map was corrected using false discovery rate (FDR, $q < 0.01$) for multiple comparisons. The voxel with the highest z value in corrected statistical inference map was defined as the coordinates of rAI (MNI coordinates: 38, 18, 2) (Figure S1, Supporting Information). In addition, we conducted reverse inference meta-analysis by using the obtained coordinates to assess whether these coordinates are reliably located in the rAI (FDR correction, $q < 0.01$). Z-scores and posterior probabilities were extracted to identify the most relevant terms in a reverse inference analysis. As indicated by z-scores and posterior probabilities, the top three terms associated with the meta-analysis included "anterior insula," "insula," and "insular," and "anterior insular," "salience network," and "anterior insula," respectively. Finally, a seed region of interest (ROI) was constructed by drawing a radius of 6 mm sphere centered on the rAI coordinates.

2.4 | dFC analysis

DFC maps were obtained using the dynamic brain connectome toolbox (DynamicBC, http://restfmri.net/forum/DynamicBC) through flexible least squares (FLS) strategy (Liao, Wu, et al., 2014). FLS approach is a data-driven method that can yield a dFC map at each time point for each scan. In brief, we first constructed a time-varying parameter regression model to characterize dynamic changes in functional connectivity:

$$y(t) = x(t)\beta(t) + u(t)$$

where $y(t)$ and $x(t)$ are the time series of seed and target regions, $u(t)$ is the approximation error, and $\beta(t)$ is the parameter which measures the covariance of the two time series and reflects the dFC between x and y at time t. Afterward, the incompatibility cost function was calculated to estimate the time-varying coefficient $\beta(t)$:

$$C(\beta, \mu, T) = \mu \cdot r_D^2(\beta, T) + r_M^2(\beta, T)$$

where $r_D^2(\beta, T)$ is the sum of squared residual dynamic error:

$$r_D^2(\beta, T) = \sum_{t=1}^{T-1} (\beta(t+1) - \beta(t))^T (\beta(t+1) - \beta(t))$$

in which the vector of coefficients $\beta(t)$ evolves slowly over time ($\beta(t+1) - \beta(t) \approx 0$). And $r_M^2(\beta, T)$ is the sum of squared residual measurement errors:

$$r_M^2(\beta, T) = \sum_{t=1}^{T} (y(t) - x(t)\beta(t))^2$$

that satisfies $y(t) - x(t)\beta(t) \approx 0$. And μ is the weighting parameter with a default value of 100 in the present study. As a result, the continuous changed model parameters $\beta(t)$ are optimally estimated to represent the dFC between seed ROI (i.e., rAI) time course and time courses of the other brain voxels at each time point (Chen et al., 2017; Liao, Wu, et al., 2014). In this case, the number of dFC maps for each participant was identical to the time points of preprocessed data. For each participant, the dFC of each voxel was then converted into Z-score by subtracting the mean value of all dFC maps and divided by the SD. This standardization procedure both reduces individual and site variability and removes the common component among dFC maps. The grand mean and variance maps of the processed dFC maps can be seen in Figure S2, Supporting Information 1.

2.5 | Dynamic states and clustering

We applied k-means clustering algorithm to all dFC maps of all subjects to obtain the different states present throughout the resting-state scan. The elbow criterion on the cluster validity index, calculating as the ratio between within-cluster distance to between-cluster distance, was used on exemplars to determine the optimal number of clusters varying k from 2 to 20, following previous dFC studies (Allen et al., 2014; Damaraju et al., 2013; Liu et al., 2016). For each subject, the exemplars were selected as windows with local maxima in FC variance. The optimal value of k ranged from 4 to 6 (Figure S3, Supporting Information 1). Bearing in mind that the previous work in neurotypical individuals identified five dynamic states of the insula subdivisions during rest (Nomi et al., 2016), a k value of 5 was adopted and we also replicated our results using values of k of 4 and 6 (Figure S4, Supporting Information 1). In brief, our k-means clustering across all subjects included two steps. The first step obtained dataset-level clustering centroids, in which k-means clustering was performed on dFC maps for each subject. A matching procedure for centroids was conducted

on all subjects with a random subject as a reference. Then, clustering centroids of all subjects were averaged as the dataset-level clustering centroids. Next, the five clustering centroids of each subject were matched with the dataset-level clustering centroids to determine the corresponding states of dFC maps. Final dynamic connectivity state maps for each subject were created by averaging dFC maps within the same state. The correlation distance was used as the similarity measurement in clustering and each *k*-means clustering was performed 10 times with random initial cluster centroids to avoid local minima (Chen et al., 2017; Damaraju et al., 2013). Reproducibility analysis using different distance functions was also established via Squared Euclidean and L1 distance, and produced similar results (Figure S4, Supporting Information 1).

To further illustrate the specificity of the rAI, an additional control analysis was also performed for the left anterior insula (MNI coordinates: −38, 18, 2). The procedures for estimating dFC and subsequent statistical analyses were identical to those used for the rAI.

2.6 | Temporal and frequency properties of dFC states

To investigate the temporal properties of dFC states, we assessed the fraction of dwell time and state transition probability of the state vector for each TD participant. The fraction of dwell time is measured as the proportion of time spent in each state. The state transition probability is the probability of transitioning from one state to another.

In the frequency spectrum analysis, global mean signals of dFC maps in each state were extracted and transformed into the frequency domain using the fast Fourier transform. We constructed the following model to characterize the relationship between frequency domain signal *y* and frequency *f*:

$$y = \frac{1}{f^{\alpha}}$$

Then, we performed logarithmic transformations on the equation to solve the frequency parameter α:

$$\log(y) = -\alpha \log(f)$$

Finally, we obtained the frequency parameters of dFC states for each TD participant and averaged them across participants to obtain a group-level α for each state. In addition, we calculated the number of peaks and troughs of the dFC time series to characterize the waveform of each state. The mode of those values was used to represent the state waveform in the TD group.

2.7 | Meta-analytic decoding of connectivity patterns in different states

To decode the potential processes associated with each distinct rAI connectivity profile, we examined the functional connectivity pattern of each dynamic state in the TD group using NeuroSynth (http://www.neurosynth.org/) (Yarkoni, Poldrack, Nichols, Van Essen, & Wager, 2011). Guided by previous work in the meta-analytic decoding of connectivity maps (Yamada et al., 2016), we first converted the original *t*-statistic maps of the TD group obtained in one-sample *t* test into *z*-statistic maps and then submitted them to the Neurosynth system for meta-analytic decoding. Next, we ranked all correlation coefficients for each state map in a descending order and identified the top five terms that showed maximum correlation with each connectivity map. Related items were incorporated into a base form to avoid reduplicative selection. Radar charts were plotted for the resulting 16 distinct terms that represent the potential psychological and physiological processes of each state.

2.8 | Statistical analyses

We used multivariate ANOVA (MANOVA) as provided by FSL's Permutation Analysis for Linear Models tool to test differences between ASD and TD groups in the five dFC states using Hotelling *T*-square statistic (Winkler et al., 2016; Winkler, Ridgway, Webster, Smith, & Nichols, 2014). Age, FIQ, mean FD, and sites (using a dummy coding scheme) were taken as covariates in the model. Prespecified brain masks were defined separately for each state using the union mask of one-sample *t*-test results for ASD and TD groups ($p < .001$, uncorrected). Nonparametric permutation testing (5,000 permutations) with threshold-free cluster enhancement inference was applied to the multivariate test and each univariate test, and the resulting voxel-wise statistical maps were corrected for familywise error rate with a significance level of $p < .05$.

2.9 | Behavioral correlations in the ASD group

We then explored the relationship between abnormal dFC values of the rAI and symptom severity as assessed by Autism Diagnostic Observation Schedule (ADOS) subscores (social interaction, communication, restricted, and repetitive behaviors) in the ASD group. Spheres with a radius of 4-mm centered on the peak coordinates of the clusters identified by MANOVA were defined as ROIs. Pearson correlation analysis was performed between the averaged signal of each ROI and ADOS subscores, with age, FIQ, mean FD, and sites (using a dummy coding scheme) as covariates. Bonferroni correction for multiple comparisons was then performed ($q < 0.05$, $p < .05/(2 \times 3) = 0.008$).

3 | RESULTS

3.1 | DFC of the rAI within each state

After *k*-means clustering, we obtained five dynamic states that are stable during the resting-state scan. The TD group showed robust functional connectivity between the rAI and diverse brain regions in each dynamic state (Figure 1a–e). In particular, transient functional connectivity associated with the rAI exhibited flexible patterns across time. In state 1, the rAI had strong connectivity with the sensorimotor regions, such as the precentral and postcentral gyrus; in state 2, the rAI exhibited connections with the occipital gyrus and dorsolateral PFC (DLPFC); in state 3, the rAI showed robust connectivity with the DLPFC and DMN regions; in state 4, the rAI had strong connections with the occipital gyrus; and in state 5, the rAI was highly connected with the DMN regions, such as the ventral mPFC (vmPFC) and PCC/precuneus.

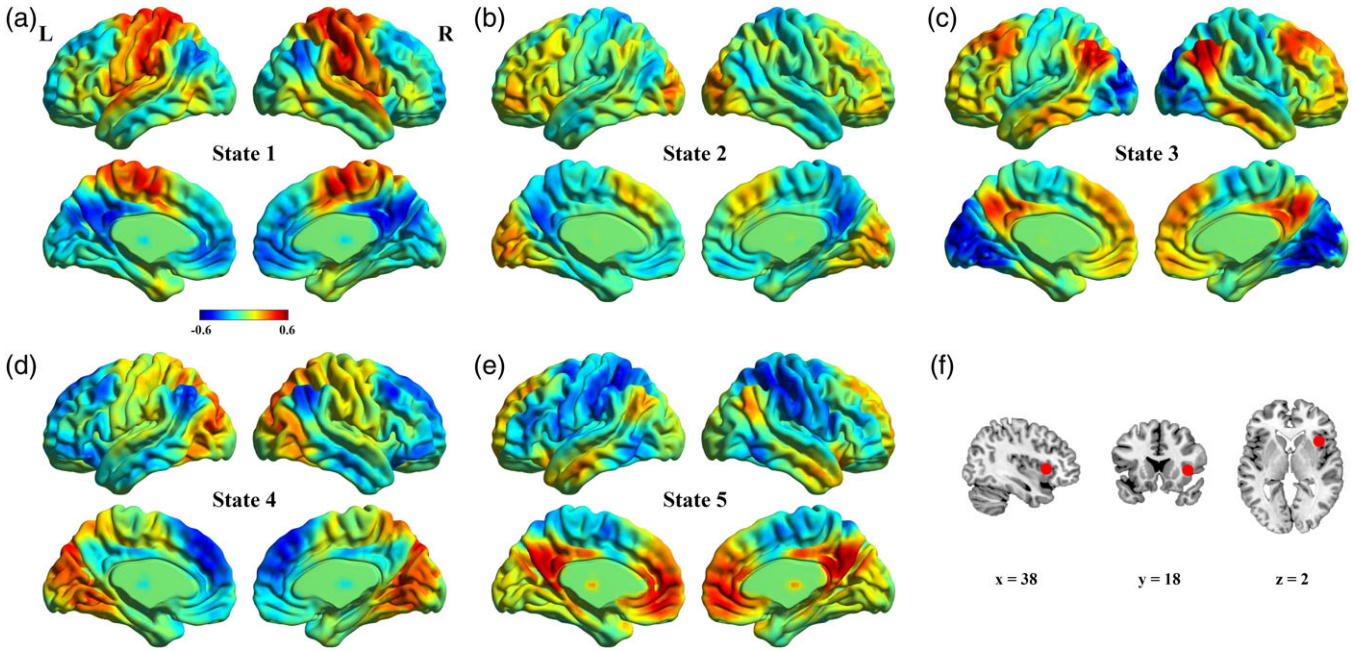

FIGURE 1 Dynamic functional connectivity (dFC) patterns of states in typically developing control group. (a–e) Mean dFC patterns between the right anterior insula (rAI) and other brain regions within each state. (f) The rAI seed [Color figure can be viewed at wileyonlinelibrary.com]

3.2 | Temporal and frequency analysis

The five dynamic states exhibited similar dwell times and frequency spectra during the scan (Figure 2a,c). However, state 3 was less likely to transition into state 4, and state 5 less likely to transition into state 1 than other transitions (Figure 2b). The most frequently occurring waveform of state 1 was with one peak and one trough. The waveform of state 4 had two peaks and two troughs. We found similar waveforms of the time series of states 2, 3, and 5 with two peaks and one trough. The diagrammatic representation of waveform for each state is plotted in Figure 2d.

3.3 | Meta-analytic decoding of dFC patterns in different states

We further investigated whether discrepancies were present in the potential psychological and physiological functions among identified dynamic states associated with the rAI. This analysis yielded 16 terms of high relevance to dFC profiles (Figure 2e). The five dynamic states exhibited different cognitive functional profiles. Functional connectivity patterns of states 1 and 4 were overlapped with the functional profiles of studies related to the sensorimotor terms, such as "somatosensory," "motor," "sensorimotor," and "visual"; state 2 showed associations with the terms related to executive terms, such as "switching," "inhibition," and "conflict"; states 3 and 5 were related to the social cognitive terms, such as "theory of mind," "self referential," "mentalizing," "social," and "emotion."

3.4 | Group differences in rAI dynamic states

Overall MANOVA results indicated significantly different dFCs associated with the rAI in vmPFC and PCC (Figure 3 and Table 2). Subsequent univariate analyses showed that those differences only occurred in two dFC states. Compared with TD individuals, ASD subjects exhibited decreased functional connectivity between rAI and vmPFC in state 3, as well as decreased connectivity with PCC in state 5. For dFC analyses with the left anterior insula as seed, no significant difference was found with the MANOVA.

In addition, to ensure that group differences in dFC were not related to head motion, we correlated mean FD values with the dFC between rAI and vmPFC and PCC, respectively. No significant correlations were found (Supporting Information 1).

3.5 | Brain–behavior analysis in the ASD group

We finally investigated the association between dFC abnormalities and ASD symptom severity. Decreased dynamic connectivity between the rAI and vmPFC in state 3 was negatively correlated with ADOS social subscore in ASD group (p = .036, uncorrected) (Figure 3b). However, this correlation did not survive Bonferroni correction for multiple comparisons.

4 | DISCUSSION

The present study investigated state-specific alterations in resting-state dFC of the rAI in ASD compared with neurotypical individuals. Characteristics of five dynamic states were first identified in TD group from multiple perspectives including temporal properties, frequency spectrum, and the potential psychological and physiological processes, to provide a complete view of each state. Then, we ascertained the brain regions and dynamic states in which ASD showed abnormal functional connectivity compared with TD. Meta-analytic decoding results revealed distinct functional profiles for the five dynamic states. Intriguingly, states 1 and 4 exhibited more associations with sensorimotor terms; state 2 had relatively more links with executive terms,

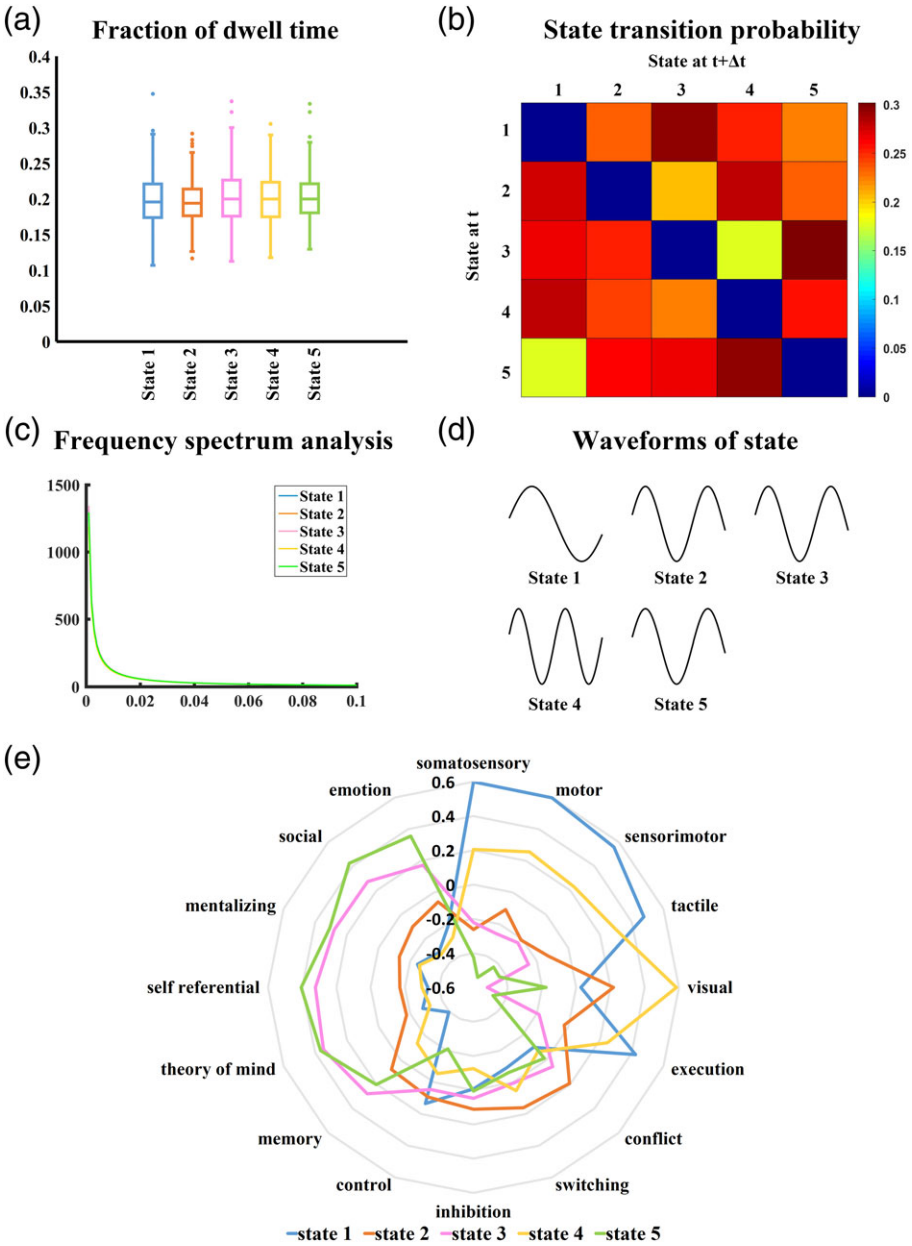

FIGURE 2 Analysis of five right anterior insula (rAI) dynamic states. (a) Fraction of dwell time. (b) State transition probability. (c) Frequency spectrum analysis. (d) Diagrammatic representation of waveform for each state. (e) Meta-analytic decoding result of each rAI dynamic state. Radar chart shows correlation coefficients for each state map with the 16 terms of interest [Color figure can be viewed at wileyonlinelibrary.com]

while states 3 and 5 showed more associations with social cognitive terms. We discovered impaired functional connectivity between the rAI and predominant hubs of DMN, including vmPFC and PCC. Compared with the TD group, the ASD group showed decreased connectivity between the rAI and these regions in states 3 and 5, but not in the other dFC states. These findings provide novel evidence for functional connectivity abnormalities relevant to the rAI in individuals with ASD from a dynamic perspective. Results also indicate the crucial role of the dFC between the rAI and DMN regions in the neural mechanisms underlying ASD.

4.1 | Dynamic states of the rAI

Across the five dynamic states, the rAI exhibited flexible functional connectivity patterns with extensive brain regions, including DMN regions, agreeing with previous reports of highly variable dynamic states of the rAI and unstable dFC between the rAI and regions of DMN in typically neurodeveloping individuals (Nomi et al., 2016). The distinguishable reoccurring functional connectivity patterns reveal different types of coordination between the rAI and other brain networks (Nomi et al., 2016). Temporal analysis in the present study also reflects different temporal properties of dFC within each state. These results demonstrate that each dynamic state of the rAI possesses a unique temporal and spatial profile. Furthermore, dynamic states associated with the rAI differentially overlapped with previous task-based studies related to psychological and physiological processing. States 1 and 4 were more linked with sensorimotor terms, and states 3 and 5 had more associations with social cognitive terms. This observation may partly uncover the potential psychological and physiological

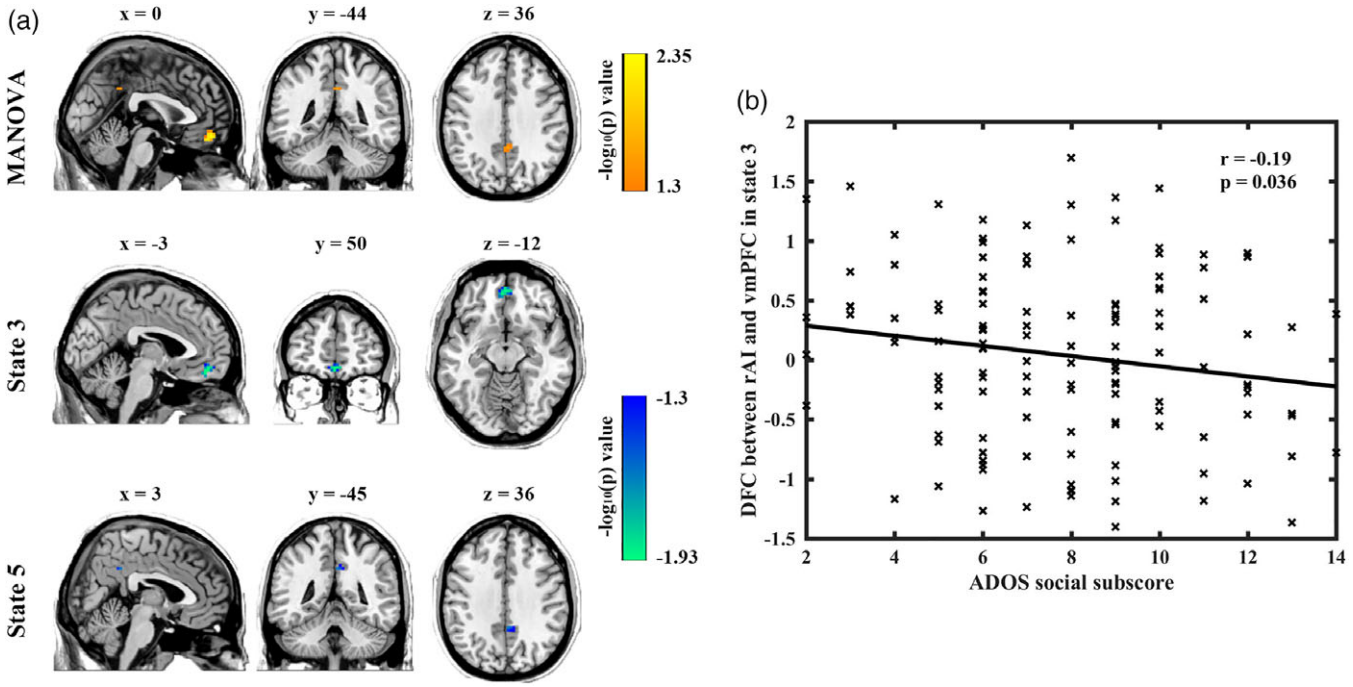

FIGURE 3 MANOVA and brain–behavior analysis results. (a) Significant group differences in the ventral medial prefrontal cortex (vmPFC) and posterior cingulate cortex (PCC) revealed by MANOVA. (b) Relationship between social subscore of ADOS and dFC between right anterior insula and vmPFC in state 3 in ASD group (uncorrected) [Color figure can be viewed at wileyonlinelibrary.com]

TABLE 2 Significant group differences in MANOVA

Brain areas	Hemi	Voxels	BA	MNI coordinates			$-\log_{10}(p)$ value
				x	*y*	*z*	
Multivariate tests							
vmPFC	L/R	39	11	0	51	−15	2.36
PCC	L/R	7	31	3	−45	36	1.59
Univariate tests							
State 3							
vmPFC	L/R	40	11	−3	45	−18	1.94
State 5							
PCC	R	7	31	3	−45	36	1.59

BA = Brodmann area; Hemi = hemisphere; L = left; MANOVA = multivariate analysis of variance; MNI = Montreal Neurological Institute; PCC = posterior cingulate cortex; R = right; vmPFC = ventral medial prefrontal cortex.

processes involved in different dFC states during the resting state (Chang, Yarkoni, Khaw, & Sanfey, 2012; Yamada et al., 2016). To the best of our knowledge, this is the first study that has applied meta-analytic methods in the study of dFC. A combination of the dynamic state analysis and meta-analytic decoding shows promise in boosting future development in dFC investigations.

4.2 | Aberrant dFC between the rAI and DMN in ASD

Referred to as the social brain areas, brain regions consisting of the DMN serve cognitive functions which are hypothesized to be involved in mentalizing, self-monitoring, and social cognition (Dante & Wim, 2013; Nathan & Grady, 2010; Susan et al., 2014). Abundant neuroimaging studies have provided support for potential links between aberrant activation and functional connectivity in the DMN associated with ASD. Individuals with ASD displayed diminished deactivation in the anterior DMN node during mentalizing tasks in comparison with a TD group (Kana et al., 2009; Kennedy, Elizabeth, & Eric, 2006). Neurotypical individuals showed more neural responses for the self-referential than for other-referential processing in the vmPFC (Lombardo et al., 2010). However, individuals with ASD showed no distinction in activating between self and others (Lombardo et al., 2010). Resting-state functional connectivity findings showed that abnormal PCC hyperconnectivity is related to the core social deficits in children with ASD (Lynch et al., 2013). An underconnectivity pattern between the anterior and posterior subnetworks of DMN was suggested to contribute to ASD symptoms in the social domain (Michal et al., 2010). Previous static functional connectivity research has also provided evidence for functional connectivity abnormalities between the rAI and regions of DMN associated with aberrant social cognitive processes in ASD (Abbott et al., 2016; von dem Hagen et al.,

2012). Nevertheless, the present study demonstrated that aberrant patterns of functional connectivity between the rAI and DMN regions are present only in some of the dFC states, and not across the whole period of the resting state. This finding poses a great challenge to previous static functional connectivity findings in ASD. It seems appropriate to conclude that the conventional static functional connectivity method is a relatively crude means of capturing the potential neurophysiological biomarkers specific to ASD; these static methods mask delicate differences among dynamic states and potentially lead to discrepant findings in neuroimaging.

Intriguingly, states in which ASD showed decreased dFC between the rAI and DMN regions were those more relevant to socio-cognitive processing implied by the meta-analytic results. These congruent relationships between functional connectivity abnormalities and cognitive functions reveal that individuals with ASD may involve inadequate spatiotemporal synchronization in states requiring high social demands. Impaired intrinsic functional connectivity between the rAI and DMN across resting-state dFC states possibly reflects brain network regulation abnormalities initiated by the rAI. These regulation abnormalities probably affect the vital role of the rAI in mediating dynamic interactions between the DMN and CEN during complex cognitive processes. These results provide new evidence for the triple-network hypothesis, which states that many psychiatric and neurological disorders are influenced by deficits in the function or connectivity of the SN, DMN, and CEN (Menon, 2011). Given the conceptual framework for the triple-network model, disrupted engagement or disengagement of the DMN modulated by signals from the rAI possibly results in aberrant self-referential mental processes in individuals with ASD. This internally oriented activity can lead to weak salience detection and reverse mapping of the SN with the consequence of further aberrant control signals to the DMN and CEN. In individuals with ASD, inappropriate internal self-referential thoughts or interpersonal social processes may be caused by aberrant dynamic interactions among the three core networks. Our findings concur with previous task-based studies on social processing. Individuals with ASD exhibited weaker cross-network interactions between the rAI and other brain systems than those in their typically developing peers in social-demanding tasks, and higher social impairments were associated with decreased connectivity during social processing (Odriozola et al., 2015). The relationships between aberrant functional circuits related to the rAI and social impairments of ASD in intrinsic states and stimulus-evoked states further highlight the potential role of the rAI in neuropathological mechanisms underlying social impairments in ASD.

The rAI region has been reported to feature significant hypoactivition during various social processes in individuals with ASD (Di Martino et al., 2009). Convergent evidence suggest that the rAI serves as an integral hub in detecting salient events and initiating network switching between the DMN and CEN through transient control signals (Menon, 2011). A previous real-time fMRI study in schizophrenia showed that improving activation in the rAI can enhance brain network connectivities associated with this region (Ruiz et al., 2013). Reduced rAI activity in ASD may result in insufficient control signals from the rAI to initiate DMN responses in social cognitive processes. Thus, individuals with ASD exhibited decreased functional interaction between the rAI and DMN in states that may more relevant to socio-cognitive processing.

4.3 | Limitations and future directions

First, the present findings were restricted to male participants. Sexual differentiation has been frequently reported in ASD at the level of cognition (Lai et al., 2012), core impairments (Van Wijngaarden-Cremers et al., 2014), genetics (Jeste & Geschwind, 2014), brain structure (Lai et al., 2013; Schaer, Kochalka, Padmanabhan, Supekar, & Menon, 2015), and functional connectivity (Alaerts, Swinnen, & Wenderoth, 2016). Given the critical role of sex in the heterogeneity of ASD (Halladay et al., 2015; Lai, Lombardo, Auyeung, Chakrabarti, & Baron-Cohen, 2015), it is imperative for future studies to disentangle the gender differences across ASD in the dFC associated with rAI. Second, although we have meta-analytically decoded the potential psychological and physiological processes of dynamic states using a data-driven approach, further task-based fMRI experiments are required to ascertain the links between cognitive functioning and each dFC state of the rAI. The current findings lay the groundwork for future dFC investigations. Third, the current dFC approach is only one of multiple methods, such as joint time–frequency analysis and dynamic graph analysis, to characterize the time-varying patterns of resting-state functional connectivity (Calhoun et al., 2014; Preti et al., 2016). Future studies may explore how to combine different dynamic connectivity methods to obtain alternative perspectives on the dFC patterns of the rAI in ASD. Finally, limitations surrounding the interpretation of ADOS scores in terms of symptom severity should also be acknowledged. It is notable that ADOS scores tend to be influenced by participant characteristics, such as age and IQ (Gotham, Pickles, & Lord, 2009; Hus, Gotham, & Lord, 2014). Although age, FIQ, mean FD, and site were taken as covariates in the brain–behavior analysis, these effects of participant characteristics cannot be completely eliminated. The use of ADOS scores in this study is problematic given that they are not reliable measures of symptom severity (Gotham et al., 2009; Hus et al., 2014). We present this analysis as a preliminary exploration of the relationship between ASD and rAI-related dFC. The results remain to be validated by future work with improved measurements of ASD symptom severity.

5 | CONCLUSION

The present study highlights abnormal dFC involving the rAI in ASD. Individuals with ASD exhibited partially decreased dynamic functional interaction between the rAI and DMN regions during the resting state. Particularly, the connectivity patterns of abnormal dFC states had increased overlap with the functional profiles of previous studies involved in social cognitive processing. Overall, these findings offer a novel perspective that deepens our understanding of ASD and suggests a potential crucial role of the functional interaction between the rAI and DMN in neurophysiological mechanisms underlying the social impairments of ASD.

ACKNOWLEDGMENTS

This work was supported by the Natural Science Foundation of China (nos. 61533006, 61673089, 81871432, and 81771919), the Specialized Research Fund for the Doctoral Program of Higher Education of China (no. 20120185110028), the Fundamental Research Funds for the Central Universities (nos. ZYGX2016J187 and 2672018ZYGX2018J079) and the Sichuan Science and Technology Program (2018TJPT0016). J.S. receives support from the National Institute for Health Research Cambridge Biomedical Resource Centre. Funding sources for the datasets comprising the 1000 Functional Connectome Project are listed at http://fcon_1000.projects.nitrc.org/fcpClassic/FcpTable.html. Funding sources for the ABIDE dataset are listed at http://fcon_1000.projects.nitrc.org/indi/abide/.

CONFLICT OF INTERESTS

None declared.

ORCID

Xujun Duan https://orcid.org/0000-0001-8543-2117

REFERENCES

Abbott, A. E., Nair, A., Keown, C. L., Datko, M., Jahedi, A., Fishman, I., & Müller, R. A. (2016). Patterns of atypical functional connectivity and behavioral links in autism differ between default, salience, and executive networks. *Cerebral Cortex*, *26*(10), 4034–4045.

Alaerts, K., Swinnen, S. P., & Wenderoth, N. (2016). Sex differences in autism: A resting-state fMRI investigation of functional brain connectivity in males and females. *Social Cognitive and Affective Neuroscience*, *11*(6), 1002–1016.

Allen, E. A., Damaraju, E., Plis, S. M., Erhardt, E. B., Eichele, T., & Calhoun, V. D. (2014). Tracking whole-brain connectivity dynamics in the resting state. *Cerebral Cortex*, *24*(3), 663–676.

American Psychiatric Association. (2013). *Diagnostic and statistical manual of mental disorders (DSM-5®)*. Arlington, VA: American Psychiatric Association.

Anderson, M. L., Kinnison, J., & Pessoa, L. (2013). Describing functional diversity of brain regions and brain networks. *NeuroImage*, *73*(8), 50–58.

Behzadi, Y., Restom, K., Liau, J., & Liu, T. T. (2007). A component based noise correction method (CompCor) for BOLD and perfusion based fMRI. *NeuroImage*, *37*(1), 90–101.

Biswal, B., Mennes, M., Zuo, X. N., Gohel, S., Kelly, C., Smith, S. M., … Colcombe, S. (2010). Toward discovery science of human brain function. *Proceedings of the National Academy of Sciences of the United States of America*, *107*(10), 4734–4739.

Biswal, B., Zerrin Yetkin, F., Haughton, V. M., & Hyde, J. S. (1995). Functional connectivity in the motor cortex of resting human brain using echo-planar MRI. *Magnetic Resonance in Medicine*, *34*(4), 537–541.

Bonnelle, V., Ham, T. E., Leech, R., Kinnunen, K. M., Mehta, M. A., Greenwood, R. J., & Sharp, D. J. (2012). Salience network integrity predicts default mode network function after traumatic brain injury. *Proceedings of the National Academy of Sciences of the United States of America*, *109*(12), 4690–4695.

Calhoun, V. D., Miller, R., Pearlson, G., & Adali, T. (2014). The chronnectome: Time-varying connectivity networks as the next frontier in fMRI data discovery. *Neuron*, *84*(2), 262–274.

Ceponiene, R., Lepistö, T., Shestakova, A., Vanhala, R., Alku, P., Näätänen, R., & Yaguchi, K. (2003). Speech-sound-selective auditory impairment in children with autism: They can perceive but do not attend. *Proceedings of the National Academy of Sciences of the United States of America*, *100*(9), 5567–5572.

Chang, L. J., Yarkoni, T., Khaw, M. W., & Sanfey, A. G. (2012). Decoding the role of the insula in human cognition: Functional parcellation and large-scale reverse inference. *Cerebral Cortex*, *23*(3), 739–749.

Chen, H., Nomi, J. S., Uddin, L. Q., Duan, X., & Chen, H. (2017). Intrinsic functional connectivity variance and state-specific under-connectivity in autism. *Human Brain Mapping*, *38*, 5740–5755.

Chevallier, C., Kohls, G., Troiani, V., Brodkin, E. S., & Schultz, R. T. (2012). The social motivation theory of autism. *Trends in Cognitive Sciences*, *16*(4), 231–239.

Craig, A. D. (2009). How do you feel--now? The anterior insula and human awareness. *Nature Reviews. Neuroscience*, *10*(1), 59–70.

Critchley, H. D., Wiens, S., Rotshtein, P., Öhman, A., & Dolan, R. J. (2004). Neural systems supporting interoceptive awareness. *Nature Neuroscience*, *7*(2), 189–195.

Damaraju, E., Allen, E. A., Belger, A., Ford, J. M., Mcewen, S., Mathalon, D. H., … Preda, A. (2013). Dynamic functional connectivity analysis reveals transient states of dysconnectivity in schizophrenia. *NeuroImage. Clinical*, *5*, 298–308.

Dante, M., & Wim, V. (2013). Emerging roles of the brain's default network. *The Neuroscientist: A Review Journal Bringing Neurobiology, Neurology, and Psychiatry*, *19*(1), 76–87.

Devue, C., Collette, F., Balteau, E., Degueldre, C., Luxen, A., Maquet, P., & Brédart, S. (2007). Here I am: The cortical correlates of visual self-recognition. *Brain Research*, *1143*, 169–182.

Di Martino, A., Ross, K., Uddin, L. Q., Sklar, A. B., Castellanos, F. X., & Milham, M. P. (2009). Functional brain correlates of social and nonsocial processes in autism Spectrum disorders: An activation likelihood estimation meta-analysis. *Biological Psychiatry*, *65*(1), 63–74.

Di Martino, A., Yan, C.-G., Li, Q., Denio, E., Castellanos, F. X., Alaerts, K., … Dapretto, M. (2014). The autism brain imaging data exchange: Towards a large-scale evaluation of the intrinsic brain architecture in autism. *Molecular Psychiatry*, *19*(6), 659–667.

Doyle-Thomas, K. A. R., Lee, W., Foster, N. E. V., Ana Tryfon, B. A., Tia Ouimet, M. A., Hyde, K. L., … Evdokia Anagnostou, M. D. (2015). Atypical functional brain connectivity during rest in autism spectrum disorders. *Annals of Neurology*, *77*(5), 866–876.

Du, Y., Pearlson, G. D., Yu, Q., He, H., Lin, D., Jing, S., … Calhoun, V. D. (2016). Interaction among subsystems within default mode network diminished in schizophrenia patients: A dynamic connectivity approach. *Schizophrenia Research*, *170*(1), 55–65.

Ebisch, S. J. H., Gallese, V., Willems, R. M., Mantini, D., Groen, W. B., Romani, G. L., … Bekkering, H. (2011). Altered intrinsic functional connectivity of anterior and posterior insula regions in high-functioning participants with autism spectrum disorder. *Human Brain Mapping*, *32*(7), 1013–1028.

Falahpour, M., Thompson, W. K., Abbott, A. E., Jahedi, A., Mulvey, M. E., Datko, M., … Müller, R. A. (2016). Underconnected, but not broken? Dynamic fcMRI shows underconnectivity in autism is linked to increased intra-individual variability across time. *Brain Connectivity*, *6*(5), 403–414.

Fox, M. D., Snyder, A. Z., Vincent, J. L., Corbetta, M., Van Essen, D. C., & Raichle, M. E. (2005). The human brain is intrinsically organized into dynamic, anticorrelated functional networks. *Proceedings of the National Academy of Sciences of the United States of America*, *102*(27), 9673–9678.

Friston, K. J., Williams, S., Howard, R., Frackowiak, R. S., & Turner, R. (1996). Movement-related effects in fMRI time-series. *Magnetic Resonance in Medicine*, *35*(3), 346–355.

Gotham, K., Pickles, A., & Lord, C. (2009). Standardizing ADOS scores for a measure of severity in autism Spectrum disorders. *Journal of Autism and Developmental Disorders*, *39*(5), 693–705.

Guo, X., Duan, X., Long, Z., Chen, H., Wang, Y., Zheng, J., … Chen, H. (2016). Decreased amygdala functional connectivity in adolescents with autism: A resting-state fMRI study. *Psychiatry Research. Neuroimaging*, *257*, 47–56.

Halladay, A. K., Bishop, S., Constantino, J. N., Daniels, A. M., Koenig, K., Palmer, K., … Singer, A. T. (2015). Sex and gender differences in autism spectrum disorder: Summarizing evidence gaps and identifying emerging areas of priority. *Molecular Autism*, *6*(1), 36.

Ham, T., Leff, A., de Boissezon, X., Joffe, A., & Sharp, D. J. (2013). Cognitive control and the salience network: An investigation of error

processing and effective connectivity. *Journal of Neuroscience*, *33*(16), 7091–7098.

He, C., Chen, Y., Jian, T., Chen, H., Guo, X., Wang, J., … Duan, X. (2018). Dynamic functional connectivity analysis reveals decreased variability of the default-mode network in developing autistic brain. *Autism Research*, in press.

Hus, V., Gotham, K., & Lord, C. (2014). Standardizing ADOS domain scores: Separating severity of social affect and restricted and repetitive Behaviors. *Journal of Autism and Developmental Disorders*, *44*(10), 2400–2412. https://doi.org/10.1007/s10803-012-1719-1

Hutchison, R. M., Womelsdorf, T., Allen, E. A., Bandettini, P. A., Calhoun, V. D., Corbetta, M., … Gonzalezcastillo, J. (2013). Dynamic functional connectivity: Promise, issues, and interpretations. *Neuroimage*, *80*(1), 360–378.

Jeste, S. S., & Geschwind, D. H. (2014). Disentangling the heterogeneity of autism spectrum disorder through genetic findings. *Nature Reviews Neurology*, *10*(2), 74–81.

Kana, R. K., Keller, T. A., Cherkassky, V. L., Minshew, N. J., & Just, M. A. (2009). Atypical frontal-posterior synchronization of theory of mind regions in autism during mental state attribution. *Social Neuroscience*, *4*(2), 135–152.

Kennedy, D. P., Elizabeth, R., & Eric, C. (2006). Failing to deactivate: Resting functional abnormalities in autism. *Proceedings of the National Academy of Sciences of the United States of America*, *103*(21), 8275–8280.

Khambhati, A. N., Sizemore, A. E., Betzel, R. F., & Bassett, D. S. (2017). Modeling and interpreting mesoscale network dynamics. *NeuroImage*, *180*(Pt B), 337–349.

Khan, A. J., Aarti, N., Keown, C. L., Datko, M. C., Lincoln, A. J., & Ralph-Axel, M. (2015). Cerebro-cerebellar resting-state functional connectivity in children and adolescents with autism Spectrum disorder. *Biological Psychiatry*, *78*(9), 625–634.

Klin, A., Jones, W., Schultz, R., Volkmar, F., & Cohen, D. (2002). Visual fixation patterns during viewing of naturalistic social situations as predictors of social competence in individuals with autism. *Archives of General Psychiatry*, *59*(9), 809–816.

Lai, M. C., Lombardo, M. V., Auyeung, B., Chakrabarti, B., & Baron-Cohen, S. (2015). Sex/gender differences and autism: Setting the scene for future research. *Journal of the American Academy of Child and Adolescent Psychiatry*, *54*(1), 11–24.

Lai, M. C., Lombardo, M. V., Ruigrok, A. N., Chakrabarti, B., Wheelwright, S. J., Auyeung, B., … Baron-Cohen, S. (2012). Cognition in males and females with autism: Similarities and differences. *PLoS One*, *7*(10), 440–440.

Lai, M. C., Lombardo, M. V., Suckling, J., Ruigrok, A. N., Chakrabarti, B., Ecker, C., … Bullmore, E. T. (2013). Biological sex affects the neurobiology of autism. *Brain*, *136*(9), 2799–2815.

Li, R., Liao, W., Yu, Y., Chen, H., Guo, X., Tang, Y. L., & Chen, H. (2018). Differential patterns of dynamic functional connectivity variability of striato–cortical circuitry in children with benign epilepsy with centrotemporal spikes. *Human Brain Mapping*, *39*(3), 1207–1217.

Liao, W., Wu, G. R., Xu, Q., Ji, G. J., Zhang, Z., Zang, Y. F., & Lu, G. (2014). DynamicBC: A MATLAB toolbox for dynamic brain connectome analysis. *Brain Connectivity*, *4*(10), 780–790.

Liao, W., Zhang, Z., Mantini, D., Xu, Q., Ji, G. J., Zhang, H., … Tian, L. (2014). Dynamical intrinsic functional architecture of the brain during absence seizures. *Brain Structure and Function*, *219*(6), 2001–2015.

Liu, F., Wang, Y., Li, M., Wang, W., Li, R., Zhang, Z., … Chen, H. (2016). Dynamic functional network connectivity in idiopathic generalized epilepsy with generalized tonic-clonic seizure. *Human Brain Mapping*, *38*(2), 957–973.

Lombardo, M. V., Bhismadev, C., Bullmore, E. T., Sadek, S. A., Greg, P., Wheelwright, S. J., … Simon, B. C. (2010). Atypical neural self-representation in autism. *Brain: A Journal of Neurology*, *133*(2), 611–624.

Lynch, C. J., Uddin, L. Q., Kaustubh, S., Amirah, K., Jennifer, P., & Vinod, M. (2013). Default mode network in childhood autism: Posteromedial cortex heterogeneity and relationship with social deficits. *Biological Psychiatry*, *74*(3), 212–219.

Marusak, H. A., Calhoun, V. D., Brown, S., Crespo, L. M., Sala-Hamrick, K., Gotlib, I. H., & Thomason, M. E. (2016). Dynamic functional connectivity of neurocognitive networks in children. *Human Brain Mapping*, *38*(1), 97–108.

Menon, V. (2011). Large-scale brain networks and psychopathology: A unifying triple network model. *Trends in Cognitive Sciences*, *15*(10), 483–506.

Menon, V., & Uddin, L. Q. (2010). Saliency, switching, attention and control: A network model of insula function. *Brain Structure and Function*, *214*(5), 655–667.

Michal, A., Kanchana, J., Calhoun, V. D., Laura, M., Stevens, M. C., Robert, S., … Pearlson, G. D. (2010). Abnormal functional connectivity of default mode sub-networks in autism spectrum disorder patients. *NeuroImage*, *53*(1), 247–256.

Spreng, R. N., & Grady, C. L. (2010). Patterns of brain activity supporting autobiographical memory, prospection, and theory of mind, and their relationship to the default mode network. *Journal of Cognitive Neuroscience*, *22*(6), 1112–1123.

Nomi, J. S., Farrant, K., Damaraju, E., Rachakonda, S., Calhoun, V. D., & Uddin, L. Q. (2016). Dynamic functional network connectivity reveals unique and overlapping profiles of insula subdivisions. *Human Brain Mapping*, *37*(5), 1770–1787.

Nomi, J. S., & Uddin, L. Q. (2015). Developmental changes in large-scale network connectivity in autism. *NeuroImage. Clinical*, *7*, 732–741.

Odriozola, P., Uddin, L. Q., Lynch, C. J., Kochalka, J., Chen, T., & Menon, V. (2015). Insula response and connectivity during social and non-social attention in children with autism. *Social Cognitive and Affective Neuroscience*, *11*(3), 433.

Power, J. D., Barnes, K. A., Snyder, A. Z., Schlaggar, B. L., & Petersen, S. E. (2012). Spurious but systematic correlations in functional connectivity MRI networks arise from subject motion. *NeuroImage*, *59*(3), 2142–2154.

Preti, M. G., Bolton, T. A., & Ville, D. V. D. (2016). The dynamic functional connectome: State-of-the-art and perspectives. *NeuroImage*, *160*, 41–54.

Ruiz, S., Lee, S., Soekadar, S. R., Caria, A., Veit, R., Kircher, T., … Sitaram, R. (2013). Acquired self-control of insula cortex modulates emotion recognition and brain network connectivity in schizophrenia. *Human Brain Mapping*, *34*(1), 200–212. https://doi.org/10.1002/hbm.21427

Satterthwaite, T. D., Wolf, D. H., Loughead, J., Ruparel, K., Elliott, M. A., Hakonarson, H., … Gur, R. E. (2012). Impact of in-scanner head motion on multiple measures of functional connectivity: Relevance for studies of neurodevelopment in youth. *NeuroImage*, *60*(1), 623–632.

Schaer, M., Kochalka, J., Padmanabhan, A., Supekar, K., & Menon, V. (2015). Sex differences in cortical volume and gyrification in autism. *Molecular Autism*, *6*(1), 1–14.

Späti, J., Chumbley, J., Brakowski, J., Dörig, N., Grosse Holtforth, M., Seifritz, E., & Spinelli, S. (2014). Functional lateralization of the anterior insula during feedback processing. *Human Brain Mapping*, *35*(9), 4428–4439.

Sridharan, D., Levitin, D. J., & Menon, V. (2008). A critical role for the right fronto-insular cortex in switching between central-executive and default-mode networks. *Proceedings of the National Academy of Sciences of the United States of America*, *105*(34), 12569–12574.

Susan, W. G., Moran, J. M., Alfonso, N. C. Ó., Christina, T., Rebecca, S., & Gabrieli, J. D. E. (2014). Associations and dissociations between default and self-reference networks in the human brain. *NeuroImage*, *111*(9), S50.

Uddin, L. Q. (2015). Salience processing and insular cortical function and dysfunction. *Nature Reviews. Neuroscience*, *16*(1), 55–61. https://doi.org/10.1038/nrn3857

Uddin, L. Q., Kinnison, J., Pessoa, L., & Anderson, M. L. (2013). Beyond the tripartite cognition–emotion–interoception model of the human insular cortex. *Journal of Cognitive Neuroscience*, *26*(1), 16–27.

Uddin, L. Q., & Menon, V. (2009). The anterior insula in autism: Underconnected and under-examined. *Neuroscience and Biobehavioral Reviews*, *33*(8), 1198–1203.

Van Wijngaarden-Cremers, P. J., van Eeten, E., Groen, W. B., Van Deurzen, P. A., Oosterling, I. J., & Van der Gaag, R. J. (2014). Gender and age differences in the core triad of impairments in autism spectrum disorders: A systematic review and meta-analysis. *Journal of Autism and Developmental Disorders*, *44*(3), 627–635.

von dem Hagen, E. A., Stoyanova, R. S., Baron-Cohen, S., & Calder, A. J. (2012). Reduced functional connectivity within and between 'social' resting state networks in autism spectrum conditions. *Social Cognitive and Affective Neuroscience*, *8*(6), 694–701.

Wager, T. D. (2011). NeuroSynth: A new platform for large-scale automated synthesis of human functional neuroimaging data. *Frontiers in Neuroinformatics*, *5*(6A), 799–801.

Wang, Y., Zhu, L., Zou, Q., Cui, Q., Liao, W., Duan, X., … Chen, H. (2018). Frequency dependent hub role of the dorsal and ventral right anterior insula. *NeuroImage*, *165*, 112–117.

Winkler, A. M., Ridgway, G. R., Webster, M. A., Smith, S. M., & Nichols, T. E. (2014). Permutation inference for the general linear model. *NeuroImage*, *92*, 381–397.

Winkler, A. M., Webster, M. A., Brooks, J. C., Tracey, I., Smith, S. M., & Nichols, T. E. (2016). Non-parametric combination and related permutation tests for neuroimaging. *Human Brain Mapping*, *37*(4), 1486–1511.

Yamada, T., Itahashi, T., Nakamura, M., Watanabe, H., Kuroda, M., Ohta, H., … Hashimoto, R.-i. (2016). Altered functional organization within the insular cortex in adult males with high-functioning autism spectrum disorder: Evidence from connectivity-based parcellation. *Molecular Autism*, *7*(1), 41.

Yan, C.-G., Cheung, B., Kelly, C., Colcombe, S., Craddock, R. C., Di Martino, A., … Milham, M. P. (2013). A comprehensive assessment of regional variation in the impact of head micromovements on functional connectomics. *NeuroImage*, *76*, 183–201.

Yan, C.-G., & Zang, Y.-F. (2010). DPARSF: A MATLAB toolbox for "pipeline" data analysis of resting-state fMRI. *Frontiers in Systems Neuroscience*, *4*, 13. https://doi.org/10.3389/fnsys.2010.00013

Yarkoni, T., Poldrack, R. A., Nichols, T. E., Van Essen, D. C., & Wager, T. D. (2011). Large-scale automated synthesis of human functional neuroimaging data. *Nature Methods*, *8*(8), 665–670.

Zhang, J., Cheng, W., Liu, Z., Zhang, K., Lei, X., Yao, Y., … Lu, G. (2016). Neural, electrophysiological and anatomical basis of brain-network variability and its characteristic changes in mental disorders. *Brain*, *139*(8), 2307–2321.

SUPPORTING INFORMATION

Additional supporting information may be found online in the Supporting Information section at the end of the article.

How to cite this article: Guo X, Duan X, Suckling J, et al. Partially impaired functional connectivity states between right anterior insula and default mode network in autism spectrum disorder. *Hum Brain Mapp*. 2019;40:1264–1275. https://doi.org/10.1002/hbm.24447